Development of Algorithms for Travel Time-Based Traffic Signal Timing, Phase I – A Hybrid Extended Kalman Filtering Approach for Traffic Density Estimation along Signalized Arterials

Final Report

Prepared by:

Henry X. Liu
Xuan Di

Department of Civil Engineering
University of Minnesota

CTS 10-10

Technical Report Documentation Page

1. Report No. CTS 10-10	2.	3. Recipients Accession No.
4. Title and Subtitle Development of Algorithms for Travel Time-Based Traffic Signal Timing, Phase I – A Hybrid Extended Kalman Filtering Approach for Traffic Density Estimation along Signalized Arterials		5. Report Date December 2010 6.
7. Author(s) Henry X. Liu and Xuan Di		8. Performing Organization Report No.
9. Performing Organization Name and Address Department of Civil Engineering University of Minnesota 500 Pillsbury Dr. S.E. Minneapolis, MN 55455		10. Project/Task/Work Unit No. CTS Project #2008074 11. Contract (C) or Grant (G) No.
12. Sponsoring Organization Name and Address Intelligent Transportation Systems Institute Center for Transportation Studies 200 Transportation and Safety Building 511 Washington Ave SE Minneapolis, MN 55455		13. Type of Report and Period Covered Final Report 14. Sponsoring Agency Code
15. Supplementary Notes http://www.cts.umn.edu/Publications/ResearchReports/		

16. Abstract (Limit: 250 words)

As technologies continue to mature, the concept of IntelliDrive has gained significant interest. Besides its application on traffic safety, IntelliDrive also has great potential to improve traffic operations. In this context, an interesting question arises: If the trajectories of a small percentage of vehicles (IntelliDrive vehicles) can be measured in real time, how can we use such data to improve traffic management? This research serves as a starting point that aims to produce a paradigm shift to optimize the traffic signal control from the use of the conventional fixed-point loop detector data to the use of mobile vehicle trajectory-based data.

Since the change of density on arterials can help traffic engineers to track the queue length at intersections, which is important for traffic signal optimization, in this project we will focus on the estimation of traffic density on urban arterials when trajectories from a small percentage of vehicles are available. Most previous work, however, focuses on freeway density estimation based merely on detector data. In this research, we adopt the MARCOM (Markov Compartment) model developed by Davis and Kang (1994) to describe arterial traffic states. We then implement a hybrid extended Kalman filter to integrate the approximated MARCOM with fixed-point and vehicle-trajectory measurements. We test the proposed model on a single signal link simulated using VisSim. Test results show that the hybrid extended Kalman filter with vehicle-trajectory data can significantly improve density estimation.

17. Document Analysis/Descriptors IntelliDrive, Trajectory control, Traffic Signal, Traffic signal control systems, Traffic density		18. Availability Statement No restrictions. Document available from: National Technical Information Services, Springfield, Virginia 22161	
19. Security Class (this report) Unclassified	20. Security Class (this page) Unclassified	21. No. of Pages 38	22. Price

Development of Algorithms for Travel Time-Based Traffic Signal Timing, Phase I – A Hybrid Extended Kalman Filtering Approach for Traffic Density Estimation along Signalized Arterials

Final Report

Prepared by:

Henry X. Liu
Xuan Di

Department of Civil Engineering
University of Minnesota

December 2010

Published by:

Intelligent Transportation Systems Institute
Center for Transportation Studies
University of Minnesota
200 Transportation and Safety Building
511 Washington Ave SE
Minneapolis, MN 55455

The contents of this report reflect the views of the authors, who are responsible for the facts and the accuracy of the information presented herein. This document is disseminated under the sponsorship of the Department of Transportation University Transportation Centers Program, in the interest of information exchange. The U.S. Government assumes no liability for the contents or use thereof. This report does not necessarily reflect the official views or policies of the University of Minnesota.

The authors, the University of Minnesota, and the U.S. Government do not endorse products or manufacturers. Any trade or manufacturers' names that may appear herein do so solely because they are considered essential to this report.

Acknowledgements

The author(s) wish to acknowledge those who made this research possible. The study was funded by the Intelligent Transportation Systems (ITS) Institute, a program of the University of Minnesota's Center for Transportation Studies (CTS). Financial support was provided by the United States Department of Transportation's Research and Innovative Technologies Administration (RITA).

Table of Contents

Chapter 1 Introduction 1
Chapter 2 Formulation of State Dynamic and Measurement Equations 3
2.1 Description of the State Space 3
2.2 Markov Compartment Model (MARCOM) 4
2.3 Approximating MARCOM Using Large Population Approximation (LPA) 6
2.4 Measurement Model 10
Chapter 3 State Estimation Using the Hybrid Extended Kalman Filter 13
Chapter 4 Numerical Examples 15
4.1 Observability 16
4.2 Estimation of Confidence Interval 16
4.3 Scenarios Analysis 18
Chapter 5 Conclusions 21
References 23

List of Figures

Figure 1. A signal link composed of n compartments 3
Figure 2. Illustration of LPA in the parking lot example 10
Figure 3. Number of vehicles in compartment 4 when penetration rate is: a)70%, b) 10%, and c) 5%, respectively. 18
Figure 4. Comparison of RMSE for different penetration rates 19

List of Tables

Table 1. Simulated parameters 15

Executive Summary

As technologies continue to mature, the concept of IntelliDrive has gained significant interest. Besides its application to traffic safety, IntelliDrive also has great potential to improve traffic operations. One significant outcome from IntelliDrive technology is the ability to estimate the trajectory of a vehicle over a short period of time (note that IntelliDrive data can be used to generate vehicle trajectories, using some post-processing algorithm, such as the Trajectory Conversion Algorithm developed by Noblis in 2007). In this context, an interesting question arises: if the trajectories of a small percentage of vehicles (IntelliDrive vehicles) can be measured in real time, how can we use such data to improve traffic management? This research serves as a starting point that aims to produce a paradigm shift to optimize the traffic signal control from the use of the conventional fixed-point loop detector data to the use of mobile vehicle trajectory-based data.

Since the change of density on arterials can help traffic engineers track the queue length at intersections, which is important for traffic signal optimization, in this project we will focus on the estimation of traffic density on urban arterials when trajectories from a small percentage of vehicles are available. Most of previous work, however, focuses on freeway density estimation based merely on detector data. In this research, we adopt the MARCOM (Markov Compartment) model developed by Davis and Kang (1994) to describe arterial traffic states. We then implement a hybrid extended Kalman filter to integrate the approximated MARCOM with fixed-point and vehicle-trajectory measurements. We test the proposed model on a single signal link simulated using VisSim. Test results show that the hybrid extended Kalman filter with vehicle-trajectory data can significantly improve density estimation.

The research findings from this project have been summarized in a paper titled "A Hybrid Extended Kalman Filtering Approach for Traffic Density Estimation along Signalized Arterials Using GPS Data" by Di, Liu, and Davis. The paper has been accepted for publication in the *Journal of Transportation Research Board: Transportation Research Record*.

Chapter 1 Introduction

Estimation of traffic densities on the freeways and arterials is critical to traffic control and management. For freeways, knowing densities for each segment can help identify bottlenecks; while densities on signalized arterials are useful to derive the queue length, which is an important index to evaluate intersection performance. Therefore, it is necessary to estimate the density evolution on arterials, so that queue dynamics at intersections can be estimated and traffic signal control can be improved.

So far most of the previous work on density estimation in a traffic dynamic system are based on “State-Space" models. A state-space model includes a dynamic equation and a measurement equation. The dynamic equation describes how the traffic system behaves and evolves, and provides prior knowledge for estimation. After the dynamic equation is set up, measurements can be used to help correct estimates and improve predictions. Szeto and Gazis *(1)* were apparently the first to use a state-space model to estimate the density, using the data from the Lincoln tunnel of the New York City.

The dynamic equation is usually in the form of first order vehicle conservation difference or differential equation. After the Cell Transmission Model (CTM) was developed by Daganzo *(2)*, several efforts concerning density estimation were built upon CTM. Munoz et al. *(3)* and Sun et al. *(4) (5)* proposed a model named the CTM-based switching mode model (SMM). To simplify the problem and maintain linearity, they make the assumption that every cell in one section has the same mode (either free flow or congestion). The mode is determined by the comparison of the predicted density with critical density. Since CTM is a deterministic model, to model the randomness of the traffic state evolution, Boel and Mihaylova *(6)*, and Sumalee et al. *(7)* added probabilistic disturbance terms to the sending and receiving functions.

Previous work on density estimation has only used detector data as measurements. IntelliDrive data (including individual vehicle location and velocity), combined with traditional detector data, can potentially be used to improve the traffic state estimation. Herrera and Bayen *(8)* applied SMM to traffic state estimation by using Lagrangian sensing data. The speed data obtained from Lagrangian sensor, however, needed to be transformed to local density before implementing SMM.

Filtering methods are used to correct the system state estimates based on measurements. The Kalman filter is the original method for state estimation. It is an optimal estimator when the system is linear, and dynamic system noise and measurement noise are Gaussian, zero-mean, and white. However, traffic systems in reality are often highly non-linear. Therefore Kalman filters

cannot be used directly for this application. To linearize the system states, a first-order approximation is applied, leading to linearized or extended Kalman filters *(1,9,10)*. The particle filter (Sequential Monte Carlo method), on the other hand, is a simulation-based method to compute the posterior distributions without a Gaussian assumption *(3,4,5,11)*.

All the models mentioned above were developed for traffic density estimation on freeways (i.e., continuous flow). Traffic state estimation on signalized arterials (i.e. interrupted flow) was largely ignored. In addition, most of the previous estimation models adopt a deterministic traffic flow model in their state equation, with white noise random error superimposed on the state equation as an exogenous item.

In this paper, we attempt to estimate traffic density along a signalized arterial, using data from both detectors and IntelliDrive. We adopt the approximating MARCOM (Markov Compartment) model developed by Davis and Kang *(9)* to describe arterial traffic states. A distinct feature of the MARCOM model consists in its inherently stochastic nature. We then develop a hybrid extended Kalman filter to integrate the density estimation from MARCOM with detector and GPS measurements.

This report is organized as follows. In Section 2, the traffic dynamic equation is described based on the approximated MARCOM model. In Section 3, we discuss how a hybrid extended Kalman filter is used to integrate the state equation with detector and IntelliDrive measurements. Numerical examples of traffic density estimation are provided in Section 4. Section 5 offers some concluding remarks and future research directions.

Chapter 2 Formulation of State Dynamic and Measurement Equations

2.1 Description of the State Space

This project focuses on a single signal link between two intersections, as shown in Figure 1. The link is divided into *n* compartments, which are numbered in ascending order from upstream to downstream. The upstream intersection is on the entrance of the first compartment, while the downstream intersection is on the exit of the last compartment. Compartments do not have to be the same length, but the length should be longer than the product of free-flow speed and time interval, which will be discussed later in Section 2.2. The state space consists of the number of vehicles in each compartment and the two boundary flows. The measurement includes input and output boundary detector counts, and space mean speed in some compartments aggregated from IntelliDrive data at certain time intervals.

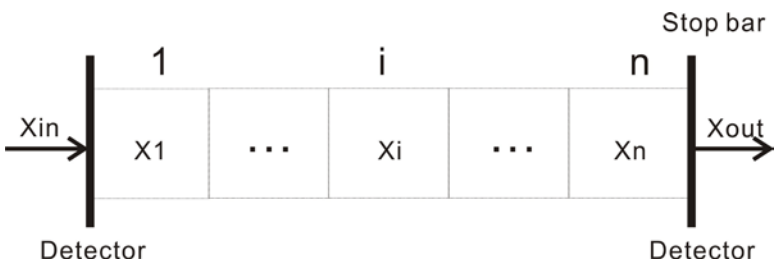

Figure 1. A signal link composed of n compartments

The state vector and measurement vector therefore can be described in Equation (1-1) and (1-2):

$$\text{state vector: } \mathbf{x}(t) = \begin{bmatrix} \mathbf{x}(t) \\ x_{in}(t) \\ x_{out}(t) \end{bmatrix}, \text{where } \mathbf{x}=(x_i) \quad i = 1, \cdots, n; \tag{1-1}$$

$$\text{measurement vector: } \mathbf{z}(t) = \begin{bmatrix} x_{in}(t) \\ x_{out}(t) \end{bmatrix}. \tag{1-2}$$

When the measured space mean speed $\overline{u}_i(t_k)$ is available for compartment *i* at time t_k, the measurement vector becomes:

$$\mathbf{z}(t_k) = \begin{bmatrix} x_{in}(t_k) \\ x_{out}(t_k) \\ \overline{u}_i(t_k) \end{bmatrix} . \qquad (1\text{-}3)$$

Here x_i is the number of vehicles in compartment i, x_{in}(t) is the cumulative arrivals passing entrance detector up to time t, x_{out}(t) is the cumulative departures passing exit detector up to time t.

2.2 Markov Compartment Model (MARCOM)

Davis and Kang *(9)* developed the MARCOM model to describe and simulate freeway traffic flow, where traffic flow is modeled as a density-dependent birth and death process. A freeway section is divided into multiple compartments and these compartments interact with their upstream and downstream ones by vehicle movements or transitions. Each vehicle is treated as a "particle" and "jumps" between compartments according to a continuous-time discrete-state Markov chain. When a vehicle makes a transition from a upstream compartment to a downstream one, a death occurs in the upstream compartment while correspondingly a birth happens in the downstream one. The transition intensity is dependent on the current population in the upstream and downstream compartments, and vehicles in each compartment are assumed to be evenly distributed. Time intervals between two consecutive transitions are assumed to be independent and exponentially distributed. When the time interval between two transitions is relatively small so that no vehicle is able to traverse the entire compartment at free-flow speed, the system maintains its Markovian property. In other words, the product of free-flow speed and transition interval must be less than the length of the compartment. It is also assumed that vehicle arrivals into the first compartment follow a Poisson arrival process.

Here we denote $q_{i-1,i}$ as the transition flow rate from upstream compartment *i-1* to downstream compartment i ($i = 2,..., n$), q_{in} as the flow entering into the first compartment, q_{out} as the flow exiting the last compartment n. Similar to Davis and Kang *(9)*, we define the transition flow rate as the product of the sending flow rate from the upstream compartment i-1 (i.e. passage intensity p_{i-1}) and non-blocking probability (nb_i) at the entrance of the downstream compartment i, as shown in Equation (2-1) and (2-2). Note that the definition of passage intensity is based on the bell-shaped flow-density fundamental diagram. From Equation (2-3), we can see that transition flow rate is dependent on both upstream number of vehicles x_{i-1} and downstream number of vehicles x_i. The transition flow rate will increase with the increase of the upstream density, and then reach a constant value, which is capacity of the upstream compartment.

$$\text{passage intensity } p_{i\text{-}1}(x_{i-1}) = \begin{cases} \dfrac{u_f x_{i-1} e^{-\frac{1}{2}\left(\frac{x_{i-1}}{x_c}\right)^2}}{L_{i-1}} & \text{if } x_{i-1} \le x_c \\ \dfrac{u_f x_c e^{-\frac{1}{2}}}{L_{i-1}} & \text{if } x_{i-1} > x_c \end{cases} \quad (i = 2, \cdots, n) \tag{2-1}$$

$$\text{non-blocking probability } nb_i(x_i) = 1 - \left(\frac{x_i}{x_{jam}}\right)^r \quad (i = 1, \cdots, n) \tag{2-2}$$

transition flow rate:

$$q_{i\text{-}1,i}(x_{i-1}, x_i) = p_{i-1}(x_{i-1}) \cdot nb_i(x_i) = \begin{cases} \dfrac{u_f x_{i-1} e^{-\frac{1}{2}\left(\frac{x_{i-1}}{x_c}\right)^2}}{L_{i-1}} \left(1 - \left(\dfrac{x_i}{x_{jam}}\right)^r\right) & \text{if } x_{i-1} \le x_c \\ \dfrac{u_f x_c e^{-\frac{1}{2}}}{L_{i-1}} \left(1 - \left(\dfrac{x_i}{x_{jam}}\right)^r\right) & \text{if } x_{i-1} > x_c \end{cases} \quad (i = 2, \cdots, n) \tag{2-3}$$

where:

$x_{i\text{-}1:}$ number of vehicles in upstream compartment *i-1*;
$x_{i:}$ number of vehicles in downstream compartment *i*;
x_c: critical density multiplied by compartment length;
x_{jam}: jam density multiplied by compartment length ($x_{jam} = 2x_c$);

$q_{i-1,i}$: transition flow rate from upstream compartment *i*-1 to downstream *i* (*i*=1,...,*n*);

u_f: free-flow speed;
r: number of lanes of the signal link;
L_i: length of compartment *i*.

For the boundary compartments, inflow and outflow rate are defined in equation (2-4) and (2-5).

$$q_{in}(x_1) = \lambda(t) \left(1 - \left(\frac{x_1}{x_{jam}}\right)^r\right) \tag{2-4}$$

$$q_{out}(x_n) = \begin{cases} \dfrac{u_f x_n e^{-\frac{1}{2}\left(\frac{x_n}{x_c}\right)^2}}{L_n} & \text{if } x_n \le x_c \text{ and traffic light is green} \\ \dfrac{u_f x_c e^{-\frac{1}{2}}}{L_n} & \text{if } x_n > x_c \text{ and traffic light is green} \\ 0 & \text{if traffic light is red} \end{cases} \tag{2-5}$$

Here $\lambda(t)$ is the arrival rate at time *t*.

Since MARCOM was developed initially for freeways, when applied to signalized intersections, the only modification is that non-blocking probability is set to be zero when the signal is red and one when it is green. It is assumed that passage intensity function (Equation (2-1)) and non-blocking probability (Equation (2-2)) are both continuously differentiable functions with respect to states. Since these two functions are not required to be continuously differentiable with respect to time, the transition intensity between compartments close to stop bar and downstream can be set to zero or one according to signal changes *(12)*.

One advantage of this model is that, instead of defining the transition flows as the minimum of the supply and demand functions as in CTM *(2)*, in MARCOM, the transition flow is a product of a passage intensity function and a non-blocking probability. Thus a continuously differentiable transition flow function can be defined, and there is no need to assume that system switches between only two modes, as in SMM *(3,4,5)*.

2.3 Approximating MARCOM Using Large Population Approximation (LPA)

The stochastic traffic dynamic process described by MARCOM is a nonlinear birth and death process, so it is difficult to integrate MARCOM directly into a filtering method. It turns out that MARCOM can be approximated as the sum of a nonlinear deterministic process (which describes the mean of the process, i.e. nominal trajectory) and a linear, time-varying Gaussian process (which describes the deviation from the mean), when the number of particles becomes large *(13,14,15)*. In other words, to apply a filtering method, we do not use MARCOM directly; instead, the deviation from the mean, which can be approximated by a linear diffusion process, is used for filtering.

To outline how this approximation can be applied, let

$$l_i = \begin{cases} -1 & \text{if a vehicle exits compartment } i \\ 1 & \text{if a vehicle enters compartment } i \\ 0 & \text{if no vehicle either enter or exit compartment } i \end{cases}$$

For example, for a road section with two compartments, a transition vector l=[-1,1,0, 0]^T would indicate a movement from compartment 1 to compartment 2, and no vehicles counted at either the entry or exit of the road section. While $q^l(\mathbf{x})$ is the transition flow rate corresponding to the transition l, say, flow from compartment 1 to compartment 2, which is a scalar dependent on state vector $\mathbf{x}$. There are three possible transitions in the two-compartment model: a vehicle enters the system, a vehicle jumps from upstream compartment 1 to downstream compartment 2, and a vehicle exits the system. Then all possible transitions with corresponding transition flow rates during unit time interval can be enumerated as:

$l_1 = \begin{bmatrix} 1 & 0 & 1 & 0 \end{bmatrix}^{\mathrm{T}}$ with transition flow $q^{l_1} = q_{\text{in}}$;

$l_2 = \begin{bmatrix} -1 & 1 & 0 & 0 \end{bmatrix}^{\mathrm{T}}$ with transition flow $q^{l_2} = q_{1,2}(x_1(t), x_2(t))$;

$l_3 = \begin{bmatrix} 0 & -1 & 0 & 1 \end{bmatrix}^{\mathrm{T}}$ with transition flow $q^{l_3} = q_{\text{out}}(x_2(t))$.

where $q_{1,2}$, q_{in} and q_{out} are defined in equations (2.3)-(2.5).

Now a vector-valued function $f(\mathbf{x})$ can be defined as the derivative of the process mean (i.e. nominal trajectory), which can be computed as the summation of transition flow rate over all the possible transitions l:

$$f(\mathbf{x}) = \frac{d\mathbf{x}}{dt} = \sum_l l \cdot q^l(\mathbf{x}). \tag{3-1}$$

And it can be further expanded in a vector format as the following:

$$f(\overline{\mathbf{x}}(t)) = \begin{bmatrix} q_{\text{in}}(\overline{x}_1(t)) - q_{1,2}(\overline{x}_1(t), \overline{x}_2(t)) \\ q_{i-1,i}(\overline{x}_{i-1}(t), \overline{x}_i(t)) - q_{i,i+1}(\overline{x}_i(t), \overline{x}_{i+1}(t)) \quad i = 2, \cdots, n-1 \\ q_{n-1,n}(\overline{x}_{n-1}(t), \overline{x}_n(t)) - q_{\text{out}}(\overline{x}_n(t)) \\ q_{\text{in}}(\overline{x}_1(t)) \\ q_{\text{out}}(\overline{x}_n(t)) \end{bmatrix} \tag{3-2}$$

For the two-compartment example discussed above, $f(\overline{\mathbf{x}}(t))$ can be written as:

$$f(\mathbf{x}(t)) = \begin{bmatrix} q_{\text{in}}(\overline{x}_1(t)) - q_{1,2}(\overline{x}_1(t), \overline{x}_2(t)) \\ q_{1,2}(\overline{x}_1(t), \overline{x}_2(t)) - q_{\text{out}}(\overline{x}_2(t)) \\ q_{\text{in}}(\overline{x}_1(t)) \\ q_{\text{out}}(\overline{x}_2(t)) \end{bmatrix}$$

After the law of large numbers is applied *(14)*, the time evolution of the process can be approximated as the solution to a system of ordinary differential equations

$$\frac{d\overline{\mathbf{x}}(t)}{dt} = f(\overline{\mathbf{x}}(t)) \tag{4}$$

where

$\overline{\mathbf{x}}(t)$: vector for the expected number of vehicles in each compartment at time t;

$f(.)$: vector-valued function defined in equation (3).

In addition, for notational convenience, we define $\mathbf{F}$ (a matrix-valued function) as the transition matrix, which is the Jacobian matrix of $f(\mathbf{x})$, with the element F_{ij} equal to the derivative of ith

element of $f(\mathbf{x})$ with respect to x_j, and $\mathbf{G}$ (a matrix-valued function) as the dynamic system noise (please see *(14)* for more details on its definition). $\mathbf{F}$ and $\mathbf{G}$ can then be written as:

$$\mathbf{F}(\mathbf{x}) = \left[\frac{\partial f_i(\mathbf{x})}{\partial x_j} \right]$$
$$\mathbf{G}(\mathbf{x}) = \sum_l l l^T q^l(\mathbf{x}). \tag{5}$$

Again, for the two-compartment example, $\mathbf{F}(\overline{\mathbf{x}}(t))$ and $\mathbf{G}(\overline{\mathbf{x}}(t))$ can be written as:

$$\mathbf{F}(\overline{\mathbf{x}}(t)) = \begin{bmatrix} \frac{\partial \dot{\overline{x}}_1(t)}{\partial x_1(t)} & \frac{\partial \dot{\overline{x}}_1(t)}{\partial x_2(t)} & 0 & 0 \\ \frac{\partial \dot{\overline{x}}_2(t)}{\partial x_1(t)} & \frac{\partial \dot{\overline{x}}_2(t)}{\partial x_2(t)} & 0 & 0 \\ \frac{\partial q_{in}(t)}{\partial x_1(t)} & \frac{\partial q_{in}(t)}{\partial x_2(t)} & 1 & 0 \\ \frac{\partial q_{out}(t)}{\partial x_1(t)} & \frac{\partial q_{out}(t)}{\partial x_2(t)} & 0 & 1 \end{bmatrix}_{\overline{\mathbf{x}}(t)} = \begin{bmatrix} \frac{\partial q_{\text{in}}}{\partial x_1} - \frac{\partial q_{1,2}}{\partial x_1} & -\frac{\partial q_{1,2}}{\partial x_2} & 0 & 0 \\ \frac{\partial q_{1,2}}{\partial x_1} & \frac{\partial q_{1,2}}{\partial x_2} - \frac{\partial q_{\text{out}}}{\partial x_2} & 0 & 0 \\ \frac{\partial q_{\text{in}}}{\partial x_1} & 0 & 1 & 0 \\ 0 & \frac{\partial q_{\text{out}}}{\partial x_2} & 0 & 1 \end{bmatrix}_{\overline{\mathbf{x}}(t)};$$

$$G(\overline{\mathbf{x}}(t)) = l_1 l_1^T q_{in} + l_2 l_2^T q_{1,2} + l_3 l_3^T q_{out}$$
$$= \begin{bmatrix} q_{in} + q_{12} & -q_{1,2} & q_{in} & 0 \\ -q_{1,2} & q_{1,2} + q_{out} & 0 & -q_{out} \\ q_{in} & 0 & q_{in} & 0 \\ 0 & -q_{out} & 0 & q_{out} \end{bmatrix}.$$

Then the difference between the system state and its deterministic approximation is a time-varying diffusion *(14)*:

$$d(\mathbf{x}(t) - \overline{\mathbf{x}}(t)) = \mathbf{F}(\overline{\mathbf{x}}(t))(\mathbf{x}(t) - \overline{\mathbf{x}}(t))dt + \mathbf{G}(\overline{\mathbf{x}}(t))^{1/2} d\mathbf{w}(t) \tag{6}$$

where $\mathbf{w}(t)$ denotes vector-valued Brownian motion, and the other notation is the same as before. Letting $\mathbf{P}(t)$ be the covariance matrix for the random vector $\mathbf{x}(t) - \overline{\mathbf{x}}(t)$, $\mathbf{P}(t)$ evolves according to the matrix Ricatti equation (1):

$$\frac{d\mathbf{P}(t)}{dt} = \mathbf{F}(\overline{\mathbf{x}}(t))\mathbf{P}(t) + \mathbf{P}(t)\mathbf{F}(\overline{\mathbf{x}}(t))^T + \mathbf{G}(\overline{\mathbf{x}}(t)) \tag{7}$$

Equations (6) and (7) demonstrate how LPA is applied to our case. General treatments of the LPA are given in Lehoczky *(13)* and Ethier and Kurtz *(14)*. A verification that the results given in Ethier and Kurtz *(14)* apply to MARCOM-type models has been given by Davis *(16)*.

Before proceeding, it may be helpful to illustrate how to use the LPA to describe the dynamic system evolution for a simple case.

Example: Consider a parking lot with 200 slots, where vehicles arrive at the lot according to a Poisson process with arrival rate λ=2.5 veh/min, and the slot occupation times are *iid* exponential random variables with a mean of 30 minutes (i.e. the departure rate is $\mu = \frac{1}{30}$ veh/min). If the lot is full when a vehicle arrives, it joins a queue and waits until a slot is available. This parking lot can be regarded as an M/M/200 queue.

The state of the above system is represented as the number of vehicles in the parking lot: x . Since there is only one compartment in this case, the state is a scalar, and the transition vector is reduced to the scalar as well. The possible transitions with corresponding transition rates during unit time interval are:

$$\begin{aligned} &l_1 = 1 \text{ with } q_{\text{in}} = \lambda \\ &l_2 = -1 \text{ with } q_{out} = x(t) \cdot \mu \end{aligned} \tag{8-1}$$

The number of vehicles in the parking lot is varying with time. But the mean can be approximated by solving:

$$\frac{d\bar{x}(t)}{dt} = f(\bar{x}(t)) = \lambda - \bar{x}(t) \cdot \mu \tag{8-2}$$

therefore $F(\bar{x}(t)) = \frac{df(\bar{x}(t))}{d\bar{x}} = -\mu$ and $G(\bar{x}(t)) = \sum l^2 q^l = \lambda + \bar{x}(t)\mu$. Consequently, the variance of *x(t)* can be approximated by solving

$$\begin{aligned} \frac{dP(t)}{dt} &= 2F(\bar{x}(t))P(t) + G(\bar{x}(t)) \\ &= -2\mu P(t) + \left(\lambda + \bar{x}(t) \cdot \mu\right) \end{aligned} \tag{8-3}$$

In this case (8-2) and (8-3) can be analytically solved as the following:

$$\bar{x}(t) = \frac{\lambda}{\mu}\left(1 - e^{-\mu t}\right) = 75\left(1 - e^{-\frac{t}{1800}}\right) \tag{8-4}$$

$$P(t) = \frac{\lambda}{\mu}\left(1 - e^{-\mu t}\right) = 75\left(1 - e^{-\frac{t}{1800}}\right) \tag{8-5}$$

The mean and variance functions can then be plotted, as shown in Figure 2. In Figure 2, the blue line is the actual number of vehicles in the parking lot generated by simulating the underlying

MARCOM birth-and-death process. The black line represents the mean of this dynamic process by using LPA. As shown in Figure 2, not only can the LPA approximation capture the stationary state, it can also describe the transient change. We can see that, despite the randomness of the actual state, it always fluctuates around the estimated mean.

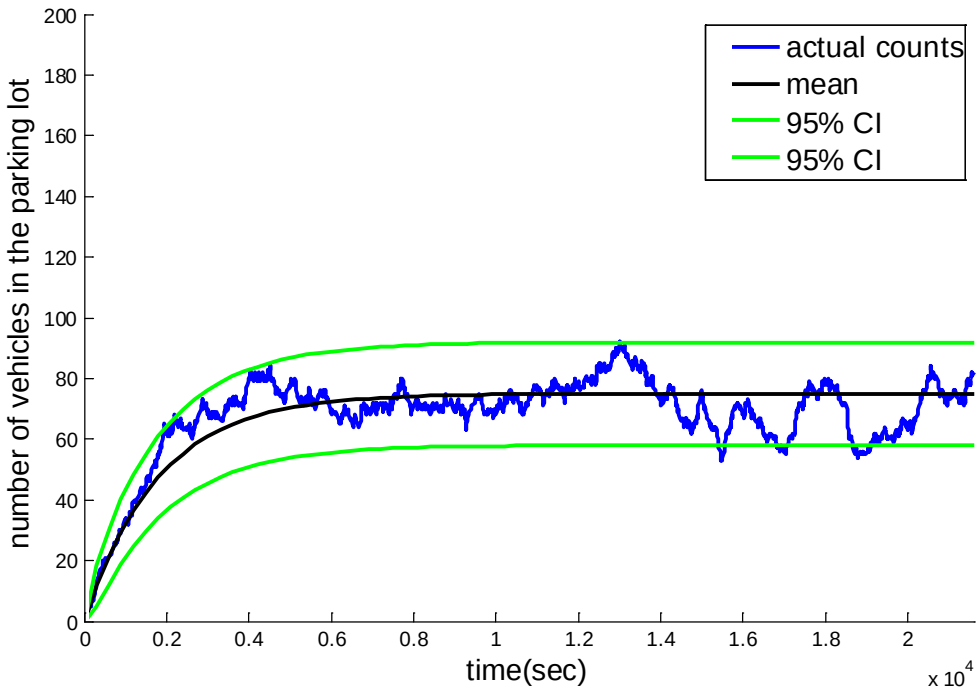

Figure 2. Illustration of LPA in the parking lot example

In this simplified parking lot model the differential equations (8-2) and (8-3) are linear so we can get the explicit formulas for the mean and the variance. In reality, many dynamic systems have nonlinear dynamics; explicit expressions for the mean and the variance cannot be easily derived but can be computed numerically.

2.4 Measurement Model

After the state dynamic model is set up, the mean dynamic traffic state of the roadway could be approximated by LPA. Meanwhile, we can obtain some observations from the field to validate and correct the dynamic model. This "prediction-correction" process could adjust the state model to fit the observations better.

We assume that, on a signal link, only boundary detector data are provided, i.e. cumulative inflow x_{in} and outflow x_{out} are measured. Besides, IntelliDrive data can provide us with additional information, such as travel times, instant speeds, etc. In this paper, vehicle speed measurements

are incorporated into the measurement equation. At certain time interval, if there are IntelliDrive-equipped vehicles running within a compartment, spot speed for each equipped vehicle within this compartment can be aggregated together to represent the average space mean speed for that compartment. If the speed obtained from IntelliDrive vehicles in this compartment is high, say, close to the free-flow speed, we know that the traffic in this compartment is performing fairly well; otherwise, congestion may happen in this compartment. Therefore, given the average speed in that compartment, we can derive the traffic density by using speed-density fundamental diagram. This could give us extra information about the traffic state of the compartment. The measurement function can be written as the following:

$$\mathbf{z}(t_k) = \mathbf{h}(\mathbf{x}(t_k)) + \mathbf{v}(t_k) \tag{9}$$

Here $\mathbf{z}(t_k)$ is the measurement vector at time t_k. $\mathbf{h}(\mathbf{x}(t_k))=[\mathbf{u}(\mathbf{x}(t_k)),\quad x_{in}(t_k),\quad x_{out}(t_k)]^T$ is the measurement function at time t_k, which is a nonlinear function of the state vector $\mathbf{x}(t_k)$.

$\mathbf{u}(\mathbf{x}(t_k))$ is the speed-density function. Its dimension is varying with time, depending on the number of compartments where we have the speed measurements. $\bar{u}_i(t_k)$ is included if speed in compartment $i\,(i=1,\cdots,n)$ is available at time t_k. We note that $\mathbf{h}(\mathbf{x}(t_k))=\left[x_{in}(t_k),\quad x_{out}(t_k)\right]^T$ when no GPS speed measurements are available. In Equation (8), $\mathbf{v}(t_k)$ is the measurement noise at time t_k (assumed to be Gaussian with mean zero and covariance $\mathbf{R}(t_k)$).

As we mentioned, $\mathbf{u}(\mathbf{x})$ is actually the density-speed function for the specified stretch of road. Here we employ bell-shaped density-speed function which was used by Davis and Kang *(9)* and Szeto and Gazis *(1)*. Since bell-shaped fundamental diagram cannot reach speed zero when density reaches the maximum, which is obviously not the case for arterials, we use a two-piece bell-shaped function as shown in Equation (10). It is easy to validate that this function is continuously differentiable.

$$\bar{u}(x) = \begin{cases} u_f e^{-\frac{1}{2}\left(\frac{x}{x_c}\right)^2} & \text{if } x \le x_c \\ 2u_f e^{-\frac{1}{2}}(1-\dfrac{x}{x_{jam}}) & \text{if } x > x_c \end{cases} \tag{10}$$

where $\bar{u}(x)$ is space mean speed, a function of the number of vehicles in the compartment, u_f is the free-flow speed, x_c is the critical density multiplied by the compartment length, and x_{jam} is the jam density multiplied by compartment length ($x_{jam}=2x_c$).

Since the measurement function $\mathbf{h}(\mathbf{x}(t_k))$ is nonlinear, it has to be linearized around a nominal trajectory $\bar{\mathbf{x}}(t)$ before a Kalman filter can be implemented. The linearized measurement matrix H is as follows:

$$\mathbf{H}(t_k) = \frac{\partial h(\mathbf{x}(t_k))}{\partial \mathbf{x}(t_k)}\Big|_{\bar{\mathbf{x}}(t_k)} = \begin{bmatrix} \frac{\partial \mathbf{u}(x(t_k))}{\partial x(t_k)} & & \\ & 1 & \\ & & 1 \end{bmatrix}_{\bar{\mathbf{x}}(t_k)} \tag{11}$$

where $\frac{\partial \mathbf{u}(x(t_k))}{\partial x(t_k)} = \left[\frac{\partial u_i(x(t_k))}{\partial x(t_k)} \right]$ when GPS measured speed $u_i(t_k)$ is available for compartment i at time t_k..

The covariance matrix $\mathbf{R}(t_k)$ of measurements represents errors caused by detector or IntelliDrive sensors. Its dimension is the same as the number of measurements obtained at time t_k and it has only non-zero elements in the diagonal. In practice, we need historical data to determine the measurement errors. However, in this paper, we assume that the speed measurement error variance is 5 $(\text{ft/s})^2$ if there is only one IntelliDrive -equipped vehicle in the compartment; If more than one IntelliDrive-equipped vehicle is running in the compartment,, the variance of the average speed should be inversely proportional to the number of vehicles, i.e. $5/m$ $(\text{ft/s})^2$, where m is the number of IntelliDrive-equipped vehicles within the compartment. In this paper, errors for cumulative flow data measured by boundary detectors are assumed to be negligible. We acknowledge that measurement errors do affect estimation results, and sensitivity analysis could be conducted to test how the estimated results vary with the change of measurement errors. But since this paper will mainly focus on the comparison of the effect of different penetration rates on the estimation accuracy, we left that for future studies.

In summary, LPA leads to the linearization of the dynamic equation, and the measurement equation can also be linearized around the nominal trajectory. After the state-space model is linearized, the hybrid extended Kalman filter (EKF) can be used to estimate the state evolution.

Chapter 3 State Estimation Using the Hybrid Extended Kalman Filter

Since traffic dynamics are non-linear, the Kalman filter (KF) should be modified before implementation. KF for non-linear systems includes Linearized KF (LKF) and Extended KF (EKF). EKF can further classified as the continuous EKF, the discrete EKF and the hybrid EKF. This paper adopts hybrid EKF for the following two reasons.

First, both LKF and EKF use the first-order approximation to transform a non-linear state-space model into a linear form, and then the Kalman filter is applied to the linear model. The difference between these two filters is that, for each updated time step, EKF utilizes *a posterior* state at time *t-1* to estimate the state at time *t*; while LKF uses pre-computed nominal trajectory for the whole time period as *a prior*. This paper utilizes EKF in place of LKF, which was used by Kang *(17)*, because pre-computed nominal trajectory is open-loop, which may lead to larger errors as time goes on. Second, the hybrid EKF must be used when we have a continuous-time system with discrete-time measurements.

The framework of how traffic state estimation works at every time step is explained as follows. The state-space model consists of the dynamic equation and measurement equation, as the following:

$$\begin{cases} \text{dynamic equation: } d(\mathbf{x}(t)-\overline{\mathbf{x}}(t)) = \mathbf{F}(\overline{\mathbf{x}}(t))(\mathbf{x}(t)-\overline{\mathbf{x}}(t))dt + \mathbf{G}(\overline{\mathbf{x}}(t))^{1/2} d\mathbf{w}(t); \\ \text{measurement equation: } \mathbf{z}(t_k) = h(\mathbf{x}(t_k)) + \mathbf{v}(t_k). \end{cases}$$

And the initial conditions are: $\mathbf{x}(0\,|\,0) = \mathbf{0},\ \mathbf{P}(0\,|\,0) = \mathbf{P}(0)$.

During the continuous time period between two consecutive measurements, i.e., when there is no measurement available, the system mean and variance can be obtained by solving equations (4) and (7). However, we should note that, when solving equations (4) and (7), the integration process starts with *a posterior* state $\mathbf{x}(t_{k-1}) = \mathbf{x}(t_{k-1}\,|\,t_{k-1})$ and covariance $\mathbf{P}(t_{k-1}) = \mathbf{P}(t_{k-1}\,|\,t_{k-1})$ at time t_{k-1}. At the end of this integration we have *a prior* state $\mathbf{x}(t_k\,|\,t_{k-1})$ and covariance $\mathbf{P}(t_k\,|\,t_{k-1})$ at time t_k *(18)*.

Once a measurement is available, the hybrid EKF can be used and Kalman gain is computed from measurement to update the system state. After updating, the mean and covariance can be re-evaluated using the latest measurement (as shown in Equation (12-6) and (12-7)). The

recursion continues until the next measurement becomes available *(19)*.

Let us denote $\delta\mathbf{x} = \mathbf{x} - \overline{\mathbf{x}}$ as the perturbation of the process from the nominal trajectory, then we have:

1. Linear perturbation prediction:

$$\delta\mathbf{x}(t_k \mid t_{k-1}) = \mathbf{F}(\mathbf{x}(t_{k-1} \mid t_{k-1})) \cdot \delta\mathbf{x}(t_{k-1} \mid t_{k-1}) \tag{12-1}$$

2. *A prior* covariance matrix:

$$\frac{d\mathbf{P}(t_k \mid t_{k-1})}{dt} = \mathbf{F}(\mathbf{x}(t_{k-1} \mid t_{k-1}))\mathbf{P}(t_{k-1} \mid t_{k-1}) + \mathbf{P}(t_{k-1} \mid t_{k-1})\mathbf{F}(\mathbf{x}(t_{k-1} \mid t_{k-1}))^T + \mathbf{G}(\mathbf{x}(t_{k-1} \mid t_{k-1})) \tag{12-2}$$

3. The Kalman gain:

$$\mathbf{K}(t_k) = \mathbf{P}(t_k \mid t_{k-1})\mathbf{H}(t_k)^T[\mathbf{H}(t_k)\mathbf{P}(t_k \mid t_{k-1})\mathbf{H}(t_k)^T + \mathbf{R}(t_k)]^{-1} \tag{12-3}$$

4. *A posterior* perturbation:

$$\delta\mathbf{x}(t_k \mid t_k) = \delta\mathbf{x}(t_k \mid t_{k-1}) + \mathbf{K}(t_k)[\mathbf{z}(t_k) - h(\mathbf{x}(t_k \mid t_{k-1})) - \mathbf{H}(t_k)\delta\mathbf{x}(t_k \mid t_{k-1})] \tag{12-4}$$

5. Nominal trajectory propogation from time t_{k-1} to t_k:

$$\frac{d\overline{\mathbf{x}}(t)}{dt} = f(\overline{\mathbf{x}}(t)) \tag{12-5}$$

6. *A posteriori* state:

$$\mathbf{x}(t_k \mid t_k) = \overline{\mathbf{x}}(t_k) + \delta\mathbf{x}(t_k \mid t_{k-1}) \tag{12-6}$$

7. *A posteriori* covariance matrix:

$$\mathbf{P}(t_k \mid t_k) = [\mathbf{I} - \mathbf{K}(t_k)\mathbf{H}(t_k)]\mathbf{P}(t_k \mid t_{k-1})[\mathbf{I} - \mathbf{K}(t_k)\mathbf{H}(t_k)]^T + \mathbf{K}(t_k)\mathbf{R}(t_k)\mathbf{K}(t_k)^T \tag{12-7}$$

where

$\delta\mathbf{x}(t_{k-1} \mid t_{k-1}), \mathbf{x}(t_{k-1} \mid t_{k-1}), \mathbf{P}(t_{k-1} \mid t_{k-1})$: *a prior* perturbation, state, covariance;

$\delta\mathbf{x}(t_k \mid t_{k-1}), \mathbf{x}(t_k \mid t_{k-1}), \mathbf{P}(t_k \mid t_{k-1})$: *a posterior* perturbation, state, covariance;

$\mathbf{F}(\mathbf{x}(t_{k-1} \mid t_{k-1}))$: transition matrix evaluated at *a posterior* state at time t_{k-1};

$\mathbf{G}(\mathbf{x}(t_{k-1} \mid t_{k-1}))$:dynamic system noise evaluated at *a posterior* state at time t_{k-1};

K: Kalman gain.

Chapter 4 Numerical Examples

To provide simulated measurements for our numerical example, we built a signalized link using the VisSim simulation model. The link is 500m long and is divided into five compartments, each of which is 100m. We place one detector at the furthest upstream boundary of the signal link and another at the furthest downstream boundary. Vehicle counts from the two detectors are collected every second, while the speed is obtained once a IntelliDrive-equipped vehicle enters the test link. Table 1 shows the simulation parameters in VisSim. It is assumed that values of arrival rate, free-flow speed, critical density and jam density are all known. In the VisSim simulation, detector counts, speed data for equipped vehicles and number of vehicles for each compartment can be obtained. The detector counts and vehicle speed are then imported to the extended Kalman filter (EKF) as input, and the EKF used to estimate the number of vehicles for each compartment. Comparing these estimates with the densities obtained from VisSim allows us to evaluate the estimation accuracy.

Table 1. Simulated parameters

Simulation time	900s
Total arrivals	280veh/900s
Arrival rate	Poisson distribution with the rate of 0.25veh/s
Signal timing	fixed, cycle length is 60s, red is 32s
Compartments length	100m/compartment, 5 compartments
Free flow speed	15m/s
Critical density	0.075veh/m/lane
Jam Density	0.15veh/m/lane

Eight scenarios are tested with different penetration rates of IntelliDrive-equipped vehicles, 100%, 90%, 70%, 50%, 30%, 10%, 5% and 0%. Boundary detector data are available for all eight scenarios. When all the vehicles are IntelliDrive-equipped (100% penetration), we know exactly how many vehicles there are in each compartment, so the measurement from 100% scenario is considered as the ground truth.

At a time instant, if there are IntelliDrive-equipped vehicles running within a compartment, the velocities of GPS-equipped vehicles within this compartment can be aggregated to approximate the space mean speed for that compartment.

$$\bar{u} = \frac{\sum_{i=1}^{n} u^i}{n_i} \tag{13}$$

where

$\bar{u}$: mean speed for IntelliDrive-equipped vehicles;

u^i : spot speed of vehicle *i*;

n_i : total amount of IntelliDrive-equipped vehicles within compartment i.

Under a scenario with higher penetration rate, the probability that one compartment contains IntelliDrive-equipped vehicles becomes larger correspondingly, thus the amount of speed measurements obtained is greater than that in lower penetration scenario. For example, under 5% scenario, most of time there is no IntelliDrive-equipped vehicle at all, then the measurement equation only includes detector count measurements.

4.1 Observability

Observability, an essential property of the dynamic system, is the issue of whether the state of a dynamic system with a known model is uniquely determinable from its inputs and outputs *(19)*. If a dynamic system is unobservable, we cannot estimate its state variables from the measurements. So the observability issue should be addressed before estimation.

For continuous-time systems, observability can be characterized by the rank of the matrix

$$\mathbf{M} = \left[\mathbf{H}^T \ \mathbf{F}^T \mathbf{H}^T \ \cdots \left(\mathbf{F}^T \right)^{n-1} \mathbf{H}^T \right],$$

where $\mathbf{F}$ is the transition matrix and $\mathbf{H}$ is the measurement matrix. Systems are observable if $\mathbf{M}$ has rank *n* (i.e. the dimension of the state vector). A computational test shows that, for a traffic system with the densities of each compartment and two boundary flows as the state space, the system is observable as long as two boundary flows and initial system conditions are given.

4.2 Estimation of Confidence Interval

Using Equations from (12-1) to (12-7), we can estimate the system mean and variance. Figure 3 shows the mean trajectories and 95% confidence intervals (CI) of the system state estimation, along with the system ground truth. In Figure 3, the solid line is the simulated number of vehicles in compartment 4 when the penetration rate is 70%, 10% and 5% respectively, dotted lines are approximated 95% confidence intervals for the estimated states, and dashed lines are system mean trajectories. For the sake of space, only results from compartment 4 are shown.

Figure 3 also demonstrates that the CI under 70% penetration rate is much tighter than that under 10% penetration rate. It suggests clearly that more information reduces the uncertainty in the estimated states. Comparison among the mean trajectories of the estimated system states also shows that 70% penetration rate has the best fit with the ground truth, but the improvement between 70% and 10% penetration rates is not significant.

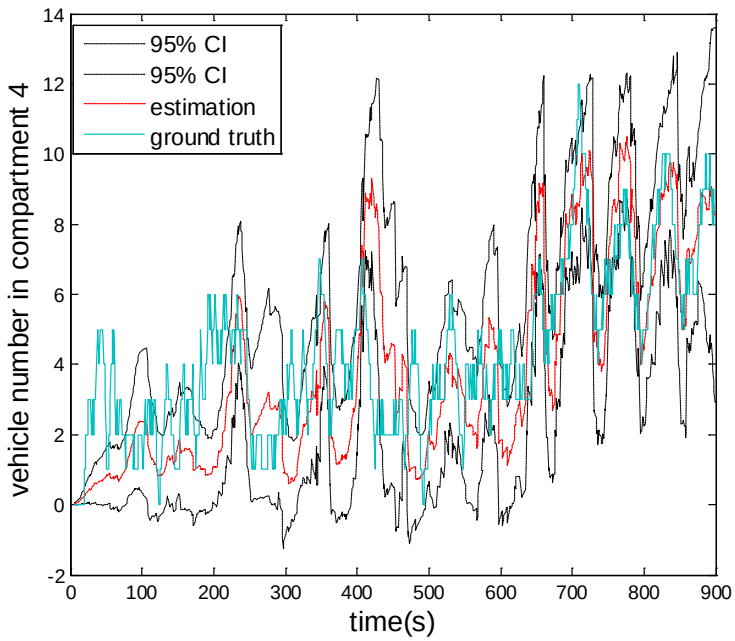

Figure 3 (a)

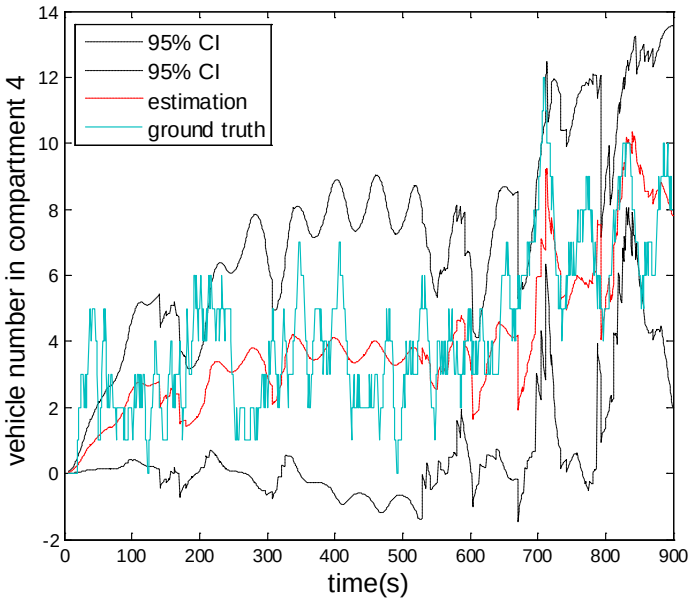

Figure 3 (b)

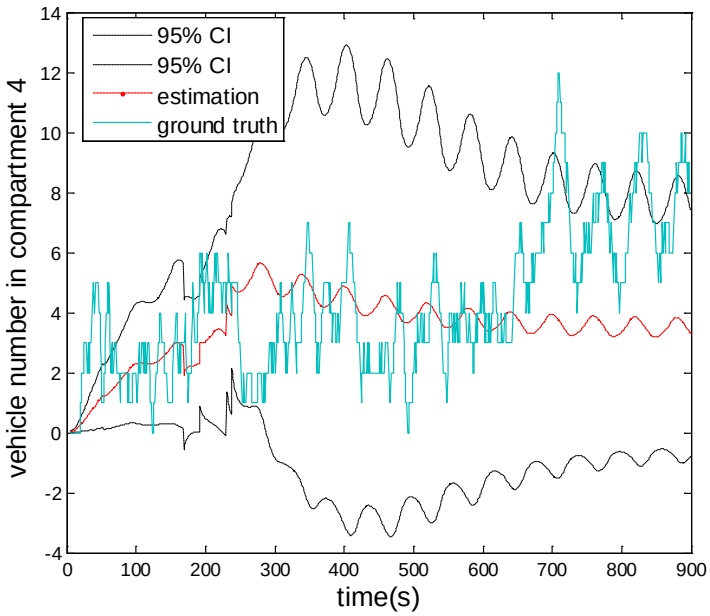

Figure 3 (c)

Figure 3. Number of vehicles in compartment 4 when penetration rate is: a) 70%, b) 10%, and c) 5%, respectively.

4.3 Scenarios Analysis

RMSE (Root Mean Square Error) is used to compare eight scenarios:

$$RMSE = \sqrt{\frac{1}{N}\sum_{t=1}^{N}(\mathbf{x}(t)-\hat{\mathbf{x}}(t))^T(\mathbf{x}(t)-\mathbf{x}(t))} \tag{14}$$

where

$\mathbf{x}(t)$: state vector;

$\hat{\mathbf{x}}(t)$: estimated state vector;

N: total simulation time;

Figure 4 show that IntelliDrive data can improve the density estimation with the higher penetration rate. But RMSE flatten out when penetration rate is greater than 10%. So for implementation purpose, this numerical example suggests that 10% is a critical penetration rate for density estimation purposes since additional IntelliDrive-equipped vehicles does not reduce the estimation error significantly.

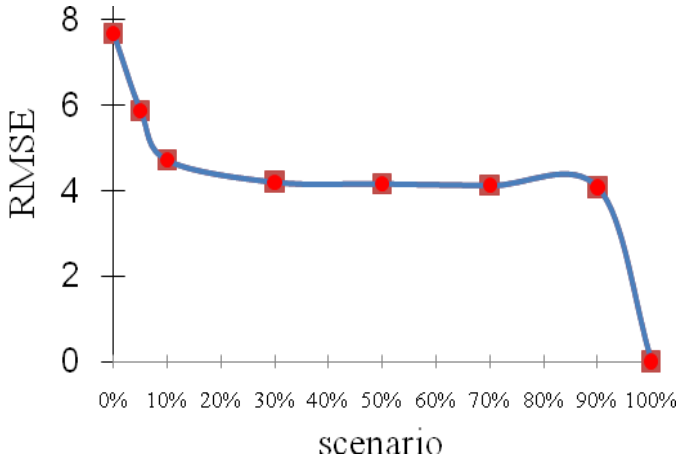

Figure 4. Comparison of RMSE for different penetration rates

Chapter 5 Conclusions

This project is among the first aiming to estimate traffic densities through the use of GPS speed data on signalized arterials. A hybrid Extended Kalman filter is adopted for density estimation. A stochastic traffic model based on vehicle conservation (MARCOM) is used as the dynamic equation, and vehicle speeds and detector counts are used as measurements. Numerical examples for a signal link with eight different penetration rates are provided. We show that higher penetration rates will lead to tighter confidence intervals and 10% penetration is critical to ensure the accuracy of density estimation.

In the future, some of the limiting assumptions made in this project should be relaxed. First, detector counts obtained from the field include both turning movement and through traffic, so turning movement needs to be estimated, together with density estimation. In principle, the MARCOM model used in this paper can deal with destination-specific estimation. Second, arrivals are assumed to follow Poisson distribution. In reality, however, vehicle arrivals at a downstream arterial link are dependent on the signal timing of the upstream intersection. One solution to this problem would be to decompose the arrivals into smaller time intervals and guarantee that within each small time interval, the vehicle arrival has the Poisson distribution, but with time-varying arrival rates. Finally, our ultimate goal is to estimate the dynamics of queuing process by using the density information. In the next step, we will refine the density estimation and compare it with field observations.

References

1. Di, X., Liu, H., and Davis, G., 2010. "A Hybrid Extended Kalman Filtering Approach for Traffic Density Estimation along Signalized Arterials Using GPS data." *Journal of Transportation Research Board, Transportation Research Record*, Accepted.

2. Szeto, M. and Gazis, D., 1972. "Application of Kalman filtering to the surveillance and control of traffic systems." *Transportation Science* 6(4), pp.419-439.

3. Daganzo, C.F., 1994. "The cell-transmission model: a dynamic representation of highway traffic consistent with the hydrodynamic theory." *Transportation Research Part B* 28(4), pp.269-288.

4. Munoz, L., Sun, X., Horowitz, R., and Alvarez, L., 2003. "Traffic density estimation with the cell transmission model." In: *Proceedings of the 2003 American Control Conference*, Denver, CO, pp.3750-3755.

5. Sun, X., Munoz, L., and Horowitz, R., 2003. "Highway traffic state estimation using improved mixture Kalman filters for effective ramp metering control." In: *Proceedings of the 42nd IEEE Conference on Decision and Control*, Maui, Hawaii, pp.6333-6338.

6. Sun, X., Munoz, L., and Horowitz, R., 2004. "Mixture Kalman filter based highway congestion mode and vehicle density estimator and its application." In: *Proceedings of the American Control Conference*, Boston, MA, pp.2098-2103.

7. Boel, R. and Mihaylova, L., 2006. "A Compositional Stochastic Model for Real Time Freeway Traffic Simulation." *Transportation Research Part B* 40(4), pp.319-334.

8. Sumalee, A., Zhong, R., Szeto, W.Y., and Pan, T., 2009. "Stochastic Cell Transmission Model: Traffic State Modeling under Uncertainties." In: *The 88th Annual Meeting of Transportation Research Board*, Washington, D.C.

9. Herrera, J.C. and Bayen, A.M., 2009. "Eulerian versus Lagrangian Sensing in Traffic State Estimation." In: *The 18th Symposium on Transportation and Traffic Theory*, Hong Kong, China.

10. Davis, G.A. and Kang, J., 1994. "Estimating Destination-specific Traffic Densities on Urban Freeways for Advanced Traffic Management." *Transportation Research Record* 1457, pp. 143-148.

11. Tampere, C.J. and Immers, L., 2007. “An Extended Kalman Filter Application for Traffic State Estimation Using CTM with Implicit Mode Switching and Dynamic Parameters.” In: *Proceedings of the IEEE Conference on Intelligent Transportation Systems*, Seattle, WA, pp.209-216.

12. Mihaylova, L. and Boel, R., 2004. “A Particle Filter for Freeway Traffic Estimation.” In: *Proceedings of the 43rd IEEE Conference on Decision and Control*, Atlantis, Paradise Island, Bahamas, pp.2106-2110.

13. Lan, C. and Davis, G., 1997. “Empirical Assessment of a Markovian Traffic Flow Model.” *Transportation Research Record* 1591, pp.31-37.

14. Lehoczky, J., 1980. “Approximations for Interactive Markov Chains in Discrete and Continuous Time.” *Journal of Mathematical Sociology* 7, 139-157.

15. Ethier, S.N. and Kurtz, T.G., 1986. *Markov Processes: Characterization and Convergence*. John Wiley & Sons, Inc., New York, NY.

16. Davis, G.A. and Nihan, N.L., 1993. “Large Population Approximations of A General Stochastic Traffic Assignment Model.” *Operations Research* 41(1), pp.169-178.

17. Davis, G.A., 2009. Course Notes for “Markov Models of Travel Demand and Traffic Flow.” Department of Civil Engineering, University of Minnesota, Minneapolis, MN.

18. Kang, J., 1995. “Estimation of Destination-specific Traffic Densities and Identification of Parameters on Urban Freeways Using Markov Models of Traffic Flow.” Ph.D. Dissertation, Department of Civil Engineering, University of Minnesota, Minneapolis, MN.

19. Simon, D., 2006. *Optimal state estimation: Kalman, H[infinity] and nonlinear approaches*. John Wiley & Sons, Inc., New York, NY.

20. Mohinder S.G. and Angus, P.A., 2008. *Kalman Filtering: Theory and Practice Using MATLAB*, third edition. John Wiley & Sons, Inc., New York, NY.